Spiculated Lesions and Architectural Distortions Detection in Digital Breast Tomosynthesis Datasets

Giovanni Palma[1,2], Isabelle Bloch[2], and Serge Muller[1]

[1] GE Healthcare, 283 rue de la minière 78530 Buc, France
[2] Télécom ParisTech (ENST) CNRS LTCI, 46 rue Barrault, 75013 Paris, France
giovanni.palma@ge.com,
isabelle.bloch@enst.fr,
serge.muller@ge.com

Abstract. Digital Breast Tomosynthesis (DBT) is a new 3D imaging technique aiming at overcoming some limitations of mammography. A computer aided detection system may help the radiologist to process the increased amount of data of this new modality. In this paper we propose to address the detection of masses and architectural distortions in DBT datasets. To achieve this task, we propose a detection scheme composed of two separate channels, each of them being dedicated to the detection of one of the target radiological signs.

We propose a description of these channels as well as a validation on clinical data. We also compare the performance with existing approaches.

1 Introduction

Mammography is a widely used technique to diagnose breast cancer. Nonetheless, due to the nature of these images, superimposition of tissues may lead to obscured lesions or false alarms. Digital Breast Tomosynthesis (DBT) is a new 3D imaging technique that potentially overcomes this limitation, but that also increases the amount of data to be reviewed by the radiologist. A computer aided detection (CAD) system dedicated to this new kind of data may help the radiologist to achieve his detection task, and increase his sensitivity.

In this paper we focus on the detection of masses and architectural distortions, which are suggestive of malignancy. This detection is performed with two independent channels, whose results are aggregated afterward. We also validate our algorithms on a database composed of 101 breast volumes (53 containing one or more biopsy proven lesions, and 48 containing no lesion).

First, we describe the method we implemented to perform the detection task, then we expose and discuss the performance the proposed approach achieved.

2 Methods

As said previously, our approach is composed of two channels dedicated to the detection of dense kernels and convergence areas, respectively. These two radiological signs are likely to represent masses and architectural distortions.

J. Martí et al. (Eds.): IWDM 2010, LNCS 6136, pp. 712–719, 2010.

2.1 Masses Detection

This channel is composed of several steps. First we process the volume slice by slice in order to detect focal-densities. This detection is performed using a fuzzy connected filter as introduced in [1], whose discriminant attributes are size, compacity and contrast-based measures. This kind of filters is suitable to mark potential masses because of their great variability. Actually, fuzzy connected filters allow to define non crisp criterion thresholds, which can help in dealing with border line structures. In the next step, the most suspicious regions are selected and grouped in 3D through a pseudo-connected component labeling. The main difference with a regular connected component labeling is that we introduce a maximum shape variability criterion to be met by the produced 3D connected components. This allows disconnecting some components and thus enables to ensure that each resulting one corresponds to only one potential lesion and does not aggregate two distinct structures together. Then for each suspicious region, the most representative slice is selected and segmented using a dynamic programming segmentation approach [2,3]. Finally, some attributes are extracted in order to feed a SVM classifier [4], which will provide the final decision: the current region is or is not suspicious. Attributes that were used mainly rely on morphological properties of the findings (compactness, size, etc.) and on statistical analysis of its neighborhood (probability of suspicious convergence, statistical measures on orientations, etc.).

2.2 Architectural Distortions Detection

The second channel aims at detecting suspicious convergence areas. In order to achieve this task, we used an a contrario modeling of the problem [5,6]. Briefly the idea is to define a convergence measure similar to the one proposed in [7] and to select realizations in real images that are unlikely to appear in healthy breasts. This last detection step is performed again slice by slice. After applying an aggregation step, a feature extraction procedure associated with a classification stage using a SVM classifier is performed. This last step is done for each slice of each finding, thus each finding is considered suspicious if at least one slice is classified as suspicious by the classifier. The features used during this classification step mainly correspond to the analysis of orientations within the neighborhood of the finding.

2.3 Final Output

The two channels previously presented aim at detecting different types of radiological signs. For this reason, a disjunctive-like aggregation step is implemented to merge their results. Nonetheless, the border between these two types of population may not be well defined. For instance, a highly spiculated mass may in certain cases be detected by the convergence detection channel. For this reason, such an aggregation strategy may improve the performance of the overall chain in comparison with a simple combination of the performance of the two channels.

3 Results

We validated the previously described CAD system on clinical DBT volumes containing biopsy proven lesions. We discuss here the performance of each channel as well as the performance of the overall system.

3.1 Database

The database we used is composed of 101 breasts, 53 with a biopsy proven cancer and 48 with no pathology. Since DBT is a relatively recent technique, this is already a quite large database. DBT volumes corresponding to these breasts were reconstructed using iterative techniques [8] from low dose projections acquired over an angular range of 40 degrees. Slice interspacing was set to 1mm. The 53 cancerous breasts contained a total of 56 lesions, 7 irregulars masses, 4 lobulated masses, 39 spiculated masses, and 3 architectural distortions. Three more lesions were discarded because they were not representative. These lesions require a dedicated detection channels to be designed when more similar data will be available. The other lesions were used to assess the performance of our detection scheme. The density detection channel was evaluated using all irregular and lobutated, as well as the less spiculated masses (29 lesions). The remaining lesions were used to compute the performance of the second channel. The choice to split the spiculated lesions into two pools has been motivated by the idea that the main characteristic of such lesions is sometimes their stellate pattern rather than their density. More practically such a choice also enables to have a more accurate validation of the convergence detection channel, even if a 13 lesions database is not enough to be actually conclusive on its real performance. But still, its allows evaluating the validity of our processing.

3.2 Masses

The performance of the channel dedicated to the detection of masses is presented trough the FROC curve of Figure 1. This curve was obtained using cross-validation techniques on the first part of the database, and corresponds to the assessment of the whole chain (marker selection and false positives reduction). More precisely, the performance of the chain was obtained using a leave-one-out strategy. During the assessment of each finding (the one left out), the classifier was trained using a n-fold procedure in order to provide a good generalization of the learning database (all the cases except the one discarded). Now from a performance stand point, depending on the user needs, several operating points can be used. For instance, we can mention that for a sensitivity of 90%, this detection scheme achieves a specificity of 1.23 false positives per volume.

An example of detection is illustrated in Figure 2. This example proposes the detection map obtained as a result of the fuzzy connected filter and the final decision obtained after false positive reduction. The intermediate result can be interpreted as follows: each pixel is associated with a gray level, which codes a membership degree (black means 0 while white means 1). This membership

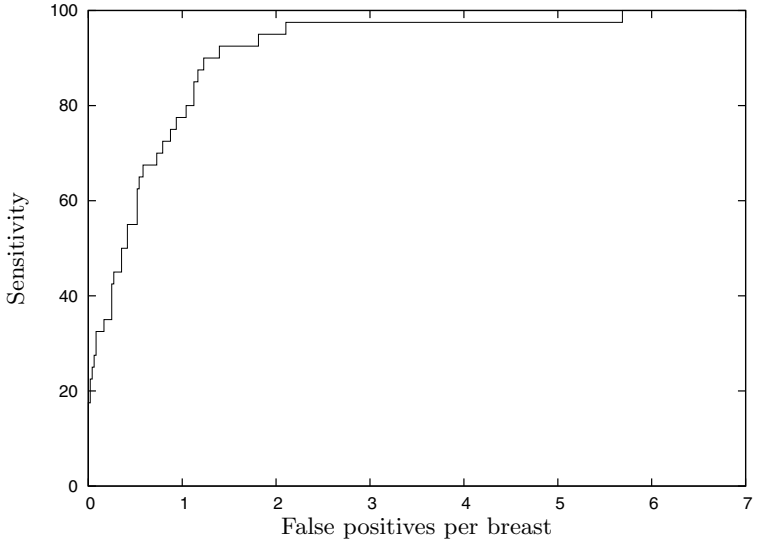

Fig. 1. FROC curve of the suspicious density detection channel

value is the degree to which the pixel is suspicious according to the filter. Now, on this particular example, we can note that the cancer is associated with a degree close but not equal to 1. This actually means that the values of the discriminant criterion were border line. Nonetheless, while the lesion does not perfectly fit the suspiciousness criterion, it is considered for further processing. The last image allows seeing the gain brought by the false positive removal stage. Here, we keep the lesion and one false positive. Let us finally state that while the example shows only one slice, 3D information is taken into account as mentioned earlier.

3.3 Convergence Patterns

The second channel was evaluated on the remaining lesions. The performance is illustrated in Figure 3. This FROC curve has also been obtained using the same cross-validation scheme as the one used for mass detection. Let us mention that this detection scheme achieved a sensitivity of 92% at 0.48 false positives per volume. However, since the amount of data is rather small, the confidence interval associated with the actual performance of this channel is probably pretty large. Nonetheless, this allows us to draw some intermediate conclusions on the validity of the approach.

An example of detection is illustrated in Figure 4. This example presents the result of the marker stage based on a contrario modeling as well as the final decision of the channel. Here the DBT slice contains an architectural distortion, which is retrieved by the marker stage and kept by the false positive removal stage. Example of false positives that are kept or suppressed during the whole processing are also provided.

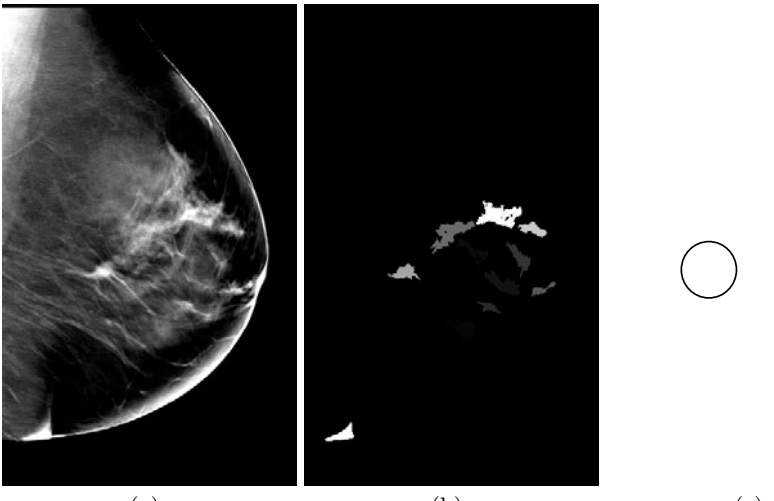

Fig. 2. Example of detection using the mass detection channel. (a) DBT slice containing a spiculated lesion. (b) Output (markers) of the fuzzy connected filter. (c) Final result: the lesion (in black) is detected as well as a false positive (in white).

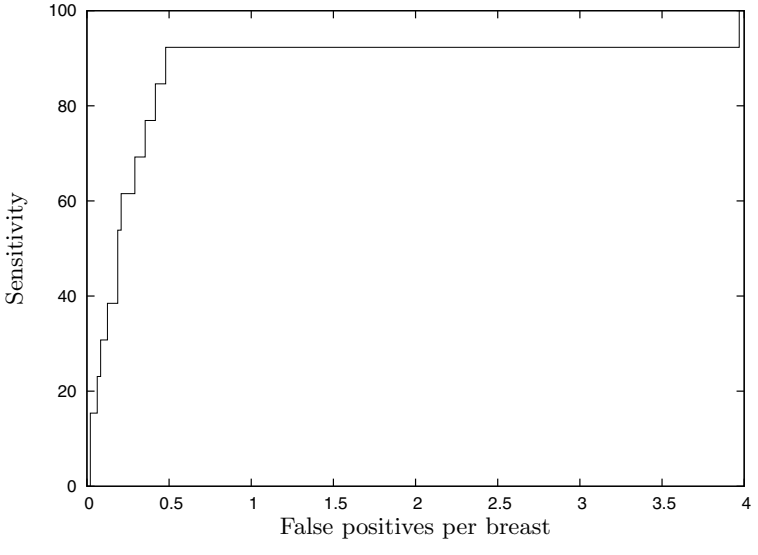

Fig. 3. FROC curve of the suspicious convergence detection channel

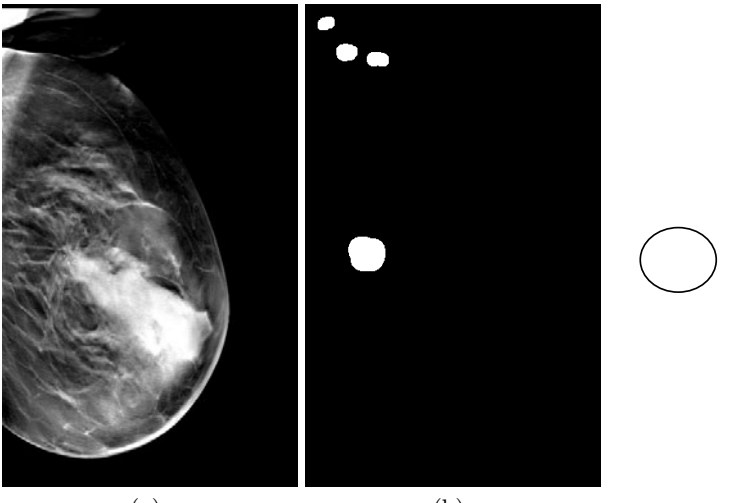

(a) (b) (c)

Fig. 4. Example of detection using the suspicious convergence detection channel. (a) DBT slice containing an architectural distortion. (b) A contrario detection result. (c) Final result: the lesion (in black) is detected as well as a false positive (in white).

3.4 Overall performances

As mentioned earlier, the target populations of the two previous channels may overlap. Table 1 presents operating points for common sensitivities, and illustrates the gain in specificity in comparison to a direct combination of the two channels performance.

The performance we obtain is comparable to other results of CAD systems for DBT datasets [9,10], while we address specifically architectural distortions in addition to masses. In [9], the authors propose a combination of detections within the projections and within the volume in order to obtain a new detection scheme. They validated it on a database containing a little bit more cancers than ours. As we can see in Table 1, our approach achieves a false positive rate of 1.31 for a 81% specificity. For similar specificity (80%), the method proposed by [9] reaches a specificity of 0.84 false positive per volume, which is better. Nonetheless, if we move to another operating point, we can get similar performances: for a sensitivity about 90%, both methods produce 1.6 false positive per breast. Now, if we increase the target sensitivity to 96%, the specificity of our approach becomes 1.81, while the performance of the other approach go beyond 2 false positives per breast. In [10], the authors propose a detection scheme whose amount of false positives is reduced using information theoretic principles. Unfortunately they only reach a sensitivity of 85% for 2.5 false positives per case.

Table 1. Performance of the combination of the two channels

Sensitivity (%)	Specificity (false positives per breast)
81,1	1,31
90,6	1,60
96,2	1,81

Nonetheless, because of the databases sizes/discrepancies, a comprehensive comparison of these approaches is hazardous. However, we can conclude that they are comparable, with a slight advantage (resp. disadvantage) of our approach for higher (resp. lower) sensitivity values, while stating validation on a larger database should be performed in order to compare them in a reliable manner.

4 Conclusion

We have introduced a new scheme for detection of some suspicious radiological signs in DBT volumes. It is composed of two distinct channels dedicated to the detection of masses and highly convergent signs, respectively. Both of them are relying on a two steps detection: a marker extraction stage followed by a false positive reduction stage. While the second step is similar for both channels, the first one is using completely different tools. Thus markers corresponding to masses are retrieved using fuzzy connected filters tools, and suspicious convergence areas are extracted using a contrario modeling based methods. We proposed a validation of the whole system and showed that its performance is comparable to other systems in the literature.

The further steps of the presented work will be to enlarge the database in order to obtain a more accurate validation. Assessing other existing approaches on such a database would enable us to actually compare them with our method. In addition to that, we would like to address other suspicious radiological signs using additional detection channels.

Acknowledgment. This work was realized under CIFRE convention 20061165 (GE Healthcare/Télécom ParisTech).

References

1. Palma, G., Bloch, I., Muller, S.: Fuzzy connected filters for fuzzy gray scale images. In: International Conference on Information Processing and Management of Uncertainty in Knowledge-Based Systems (IPMU), Malaga, Spain, June 2008, pp. 667–674 (2008)
2. Timp, S., Karssemeijer, N.: A new 2D segmentation method based on dynamic programming applied to computer aided detection in mammography. Medical Physics 31(5), 958–971 (2004)

3. Apffel, L., Palma, G., Muller, S., Bloch, I.: Fuzzy segmentation of masses in digital breast tomosynthesis images based on dynamic programming. In: International Conference on Imaging Theory and Applications (IMAGAPP), Angers, France (June 2010)
4. Vapnik, V.N.: The nature of statistical learning theory. Springer, New York (1995)
5. Palma, G., Muller, S., Bloch, I., Iordache, R.: Convergence areas detection in digital breast tomosynthesis volumes using a contrario modeling. In: SPIE Symposium on Medical Imaging, Lake Buena Vista, FL, USA (February 2009)
6. Palma, G., Muller, S., Bloch, I., Iordache, R.: Fast detection of convergence areas in digital breast tomosynthesis. In: IEEE International Symposium on Biomedical Imaging (ISBI), Boston, MA, USA, June 2009, pp. 847–850 (2009)
7. Karssemeijer, N., te Brake, G.M.: Detection of stellate distortions in mammograms. IEEE Transactions on Medical Imaging 5(5), 611–619 (1996)
8. Andersen, A.H., Kak, A.C.: Simultaneous algebraic reconstruction technique (SART): A superior implementation of the ART algorithm. Ultrasonic Imaging 6(1), 81–94 (1984)
9. Chan, H.P., Wei, J., Zhang, Y., Helvie, M.A., Moore, R.H., Sahiner, B., Hadjiiski, L., Kopans, D.B.: Computer-aided detection of masses in digital tomosynthesis mammography: Comparison of three approaches. Medical Physics 35(9), 4087–4095 (2008)
10. Singh, S., Tourassi, G.D., Baker, J.A., Samei, E., Lo, J.Y.: Automated breast mass detection in 3D reconstructed tomosynthesis volumes: A featureless approach. Medical Physics 35(8), 3626–3636 (2008)